ENVIRONMENTAL RESEARCH
COMMUNICATIONS

INCLUSIVE PUBLISHING
TRUSTED SCIENCE

Part of the
ENVIRONMENTAL RESEARCH
SERIES

PURPOSE-LED
PUBLISHING™

PAPER • **OPEN ACCESS**

Short-term energy and meteorological impacts on Thanksgiving CO_2 in Salt Lake City

To cite this article: Ju-Mee Ryoo *et al* 2025 *Environ. Res. Commun.* **7** 065001

Environmental Research Communications

PAPER

Short-term energy and meteorological impacts on Thanksgiving CO_2 in Salt Lake City

Ju-Mee Ryoo[1,2], **Inez Fung**[3,4] and **James R Ehleringer**[5]

[1] Atmospheric Science Branch, Earth Science Division, NASA Ames Research Center, Moffett Field, CA 94035, United States of America
[2] Bay Area Environmental Research Institute, Moffett Field, CA 94035, United States of America
[3] Department of Earth and Planetary Science, University of California, Berkeley, Berkeley, CA 94720, United States of America
[4] Department of Environmental Science, Policy and Management, University of California, Berkeley, Berkeley, CA 94720, United States of America
[5] Department of Biology, University of Utah, Salt Lake City, UT 84112, United States of America

E-mail: ju-mee.ryoo@nasa.gov

OPEN ACCESS

RECEIVED
29 July 2024

REVISED
22 March 2025

ACCEPTED FOR PUBLICATION
6 May 2025

PUBLISHED
2 June 2025

Keywords: Thanksgiving holidays, Vulcan3 onroad and non-onroad emission, meteorology, Salt Lake City CO_2 in-situ measurement, factor analysis

Supplementary material for this article is available online

Abstract

Long-term, high-frequency atmospheric CO_2 measurements at multiple sites in Salt Lake City (SLC), Utah, reveal that annual and monthly CO_2 variability aligns with a priori estimates of emissions from anthropogenic and biological sources. In this study, we investigate whether short-term fluctuations in anthropogenic emissions, as captured in the Vulcan3 dataset for the United States, can be detected in atmospheric CO_2 observations. Specifically, we focus on Thanksgiving holidays, when traffic and energy usage patterns differ from the rest of November. Onroad CO_2 emissions exhibit a double peak during weekday morning and evening rush hours but remain relatively low on weekends and Thanksgiving. Interestingly, CO_2 mole fractions during Thanksgiving were higher than the rest of November at all SLC monitoring sites, particularly from 2008 to 2013. This increase is partially attributed to elevated energy-related emissions — especially residential sources — and meteorological factors such as weak wind speeds, cold temperature, and a low planetary boundary layer height (PBLH). While CO_2 emissions and mole fraction patterns align over time, notable spatial differences exist. For instance, the near-highway site in Murray shows the highest CO_2 mole fractions despite low local emissions, suggesting pollution transport via highways and wind advection. Random Forest model-based SHapley Additive exPlanations (SHAP) analysis reveals that onroad emissions dominate CO_2 contributions on weekdays and weekends, while energy-related emissions play a larger role during Thanksgiving, alongside meteorological drivers such as wind speed and PBLH. Across six urban cities, CO_2 emissions display a consistent pattern: residential and commercial emissions peak during Thanksgiving with substantial year-to-year variability, while onroad emissions peak during weekdays, with minimal variability. These findings highlight that urban CO_2 variability is driven by the combined influence of emissions and meteorology, underscoring the need for integrated mitigation strategies. Additionally, multi-site measurements are essential for accurate source attribution and effective policy interventions.

1. Introduction

Urban areas significantly contribute to anthropogenic CO_2 emissions, resulting in elevated CO_2 levels and temperature compared to global averages (International Energy Agency 2008, Gurney *et al* 2015, Umezawa *et al* 2020, Yin *et al* 2023). Consequently, understanding and monitoring urban CO_2 emissions, as well as their connection to human behavior, are essential for gaining insights into global CO_2 cycles (Rosenzweig *et al* 2010,

Wofsy *et al* 2010a, 2010b, Hutyra *et al* 2014). Over the past two decades, extensive high-frequency measurements have been conducted in Salt Lake City (SLC), Utah, USA (Pataki *et al* 2003, 2006, Ehleringer *et al* 2008, 2009, Strong *et al* 2011, McKain *et al* 2012, Lin *et al* 2018, Mitchell *et al* 2018, Mallia *et al* 2023). These measurements provide valuable 'top-down' data for characterizing urban atmospheric CO_2 and corroborating bottom-up emissions estimates derived from categorized emitting sources and established algorithms.

Urban CO_2 levels are subject to influences from various factors, encompassing meteorological, biological, and anthropogenic processes (Strong *et al* 2011, McKain *et al* 2012, Hutyra *et al* 2014, Gualtieri *et al* 2021). Previous studies have used ground-based measurements and high-resolution atmospheric transport models to investigate greenhouse gas emissions and CO_2 mole fractions in urban areas (Newman *et al* 2013, Mitchell *et al* 2018, Agustí-Panareda 2019). For example, Newman *et al* (2013), using data from the CalNex-LA ground campaign and the WRF-STILT model (Weather Research and Forecasting—Stochastic Time-Inverted Lagrangian Transport), found that local fossil fuel combustion contributed approximately 50% to overnight CO_2 enhancements and up to ~100% during midday over Los Angeles in the spring. Agustí-Panareda (2019) further demonstrated that increasing horizontal resolution is critical for modeling 'CO_2 weather,' as it improves the surface representation of both wind patterns and CO_2 fluxes. Within SLC, CO_2 mole fractions exhibit significant sensitivity to emissions, atmospheric stability, capping inversions, and planetary boundary layers (PBL), especially under stable conditions (Pataki *et al* 2005, Ehleringer *et al* 2008). Moreover, factors such as traffic density, natural gas heating, land cover, climate, and seasonal variations exert substantial influence on urban CO_2 fluxes (Day *et al* 2002, Wentz *et al* 2002, Nowak *et al* 2002, Apadula *et al* 2003, Nasrallah *et al* 2003, Gratani and Varone 2005). Isotopic analyses performed in SLC have further elucidated the contributions of gasoline and natural gas combustion to CO_2 sources, while also highlighting periods when photosynthesis serves as a minor CO_2 sink (Pataki *et al* 2003, 2006). A recent study by Cobo *et al* (2024) demonstrated that the drying of the Great Salt Lake is a significant source of anthropogenic GHG emissions in the SLC region. The study emphasizes that climate change exacerbates drought in arid areas like SLC, highlighting the importance of including such factors in GHG assessments and emission reduction strategies.

Numerous studies have underscored the direct impact of human activities on urban CO_2 emissions using high resolution 'bottom-up' CO_2 inventory data such as Hestia product (Gurney *et al* 2012, Patarasuk *et al* 2016, Kunik *et al* 2019) and Vulcan version 3 (Vulcan3) dataset (Gurney *et al* 2019, 2020). Notably, traffic congestion, especially during peak rush hours, emerges as a significant driver of CO_2 emissions (Barth and Boriboonsomsin 2008, Hutyra *et al* 2014, Turner *et al* 2020, Venturi *et al* 2021, Wu *et al* 2021, Ray *et al* 2022, Mallia *et al* 2023). Emission factor curves, which are contingent upon vehicle speed, exhibit a distinct parabolic shape characterized by elevated emission rates at both high and low speeds, with a minimum emission rate occurring at moderate speeds (Barth and Boriboonsomsin 2008). This highlights the sensitivity of CO_2 emissions to driving patterns and traffic conditions.

Recent investigations conducted during the COVID-19 pandemic documented a substantial reduction in anthropogenic CO_2 emissions, approximately 30% lower, primarily attributed to alterations in traffic (48%) and non-traffic emissions (8%) (Turner *et al* 2020). Mallia *et al* (2023) also showed that reductions in CO_2 emissions were observed over the downtown SLC, near major roadways, and potentially at industrial point sources over March-April 2020 during the COVID-19 lockdown. However, while these studies primarily aim to identify predominant anthropogenic CO_2 sources during different diurnal periods and their variations in response to various human activities, they do not explore additional factors, such as the relative contribution of meteorological conditions that might explain short-term fluctuations in CO_2 levels in SLC.

This study utilizes multi-year, high-frequency surface-based observations covering weekdays, weekends, and Thanksgiving holidays, revealing distinct CO_2 variations across these occasions. To complement these observations, we incorporate meteorological data and bottom-up inventory CO_2 emission data. Here we compare observed CO_2 mole fraction variations and assess whether emission patterns during Thanksgiving resemble those on other days across different cities. To quantify the relative contributions of meteorological variables and emissions to CO_2 mole fractions, we apply a Random Forest (RF) model-based SHapley Additive exPlanations (SHAP) analysis (Shapley 1953, Lundberg *et al* 2020, Nelson *et al* 2023). Our focus is specifically on the Thanksgiving holidays, when traffic patterns and energy usage are expected to differ significantly from the rest of November. This study addresses two key objectives:

1. **Identify** short-term fluctuations in CO_2 mole fractions and emissions across weekdays, weekends, and Thanksgiving, and explain the observed differences.
2. **Examine** contributing factors, including meteorology and anthropogenic emissions (onroad and energy-related), that drive short-term CO_2 variability.

The paper is organized as follows: Section 2 outlines the dataset and methodology. Section 3 presents the characteristics of CO_2 mole fractions, emission types by sectors, and meteorological influences over the SLC, along with the relative contributions of each factor to CO_2. Section 4 discusses CO_2 emission characteristics during different occasions to see any consistent patterns across other urban cities. Conclusions follow in section 5.

2. Data and methodology

Our analysis focuses on high-frequency CO_2 variations from the Utah Urban Carbon Dioxide Network (UUCON) centered around Salt Lake City (SLC, Lin *et al* 2018) from 2008 to 2019, encompassing weekdays, weekends, and Thanksgiving holidays. To ensure the robustness of our findings, we compare meteorological influences on CO_2 patterns between two periods: 2008–2013 and 2014–2019. Since anthropogenic CO_2 emission data from the Vulcan3 dataset (Gurney *et al* 2019, 2020) is available only for 2010–2015, emission analysis is performed during this period.

In this study, the term 'Thanksgiving' refers to a six-day period encompassing Tuesday through Sunday in the third week of November. No large sensitivity was found whether we consider a three-day or five-day interval, but variations in energy use and distinctions in meteorological conditions become more pronounced when we analyze data from a few days before and after the holidays, facilitating clearer comparisons with other periods. 'Weekday' and 'Weekend' refer to weekdays and weekends in November. To obtain results from distinct occasions, we ensured no overlap between weekdays, weekends, and Thanksgiving days.

2.1. High-frequency CO_2 and meteorological data

We utilized hourly averaged CO_2 mole fraction data from the five UUCON sites (Bares *et al* 2019) for November weekday, weekend, and Thanksgiving days from 2008 to 2019. Data were from five sites: Rose Park (111.92°W, 40.78°N, RPK), Murray (111.89°W, 40.66°N, MUR), Sugar House (111.86°W, 40.73°N, SUH), the University of Utah (111.85°W, 40.76°N, UOU), and Daybreak (112.07°W, 40.54°N, DBK). The locations of these sites are displayed on figure 1(a). The hourly CO_2 mole fractions during 2008–2019 for those sites show increasing trends for all sites (Mitchell *et al* 2018), as shown in figure S2. Our study period covers CO_2 mole fraction data from various periods, as some data are missing from some sites:

- **RPK:** November 2009–2019
- **MUR:** November 2008–2012
- **DBK:** November 2008–2019 (with gaps in 2012 and 2013)
- **UOU & SUG:** November 2008–2019

Since the surface meteorological data at the exact CO_2 measurement site were not available from the MesoWest data archive (Horel *et al* 2002), the sub-hourly meteorological data closest to each CO_2 measurement site, including wind direction and speed, relative humidity, and surface temperature, were obtained from 2008–2019. For example, as meteorological data, we used the surface measurement at KSLC (111.97°W, 40.77°N) for Rose Park, UT12 (111.90°W, 40.64°N) for Murray, UT23 (111.90°W, 40.72°N) for Sugar House, WBB (111.85°W, 40.766°N) for University of Utah, and TRJO (112.06°W, 40.56°N) for Daybreak. The sub-hourly data are averaged to hourly intervals in local standard time for comparison with CO_2 measurements. The wind patterns at the site are shown in figure 1(b). Although wind speed varies from year to year, the wind direction has remained relatively consistent. Therefore, the overall distribution of wind measurements did not differ significantly from year to year (not shown).

We also estimated the planetary boundary layer height (PBLH) using the parcel method (Holzworth 1964). This method determines the PBLH by identifying the altitude where the observed hourly surface temperature profile intersects the dry adiabatic lapse rate. The hourly surface temperature data were acquired from Weather Underground, while temperature and pressure vertical profiles at 12Z were obtained from atmospheric sounding data at Salt Lake City International Airport (40.79°N, 111.98°W), provided by the University of Wyoming Atmospheric Sounding Site. The parcel method is widely used for estimating PBLH, primarily relying on the thermodynamic characteristics from radiosonde profiles. Compared to other PBLH detection methods, it exhibits distinct and consistent diurnal and seasonal variations (Seidel *et al* 2010). This approach has been extensively employed in air quality studies in SLC (Strong *et al* 2011) and other urban valley regions (Ryoo *et al* 2019).

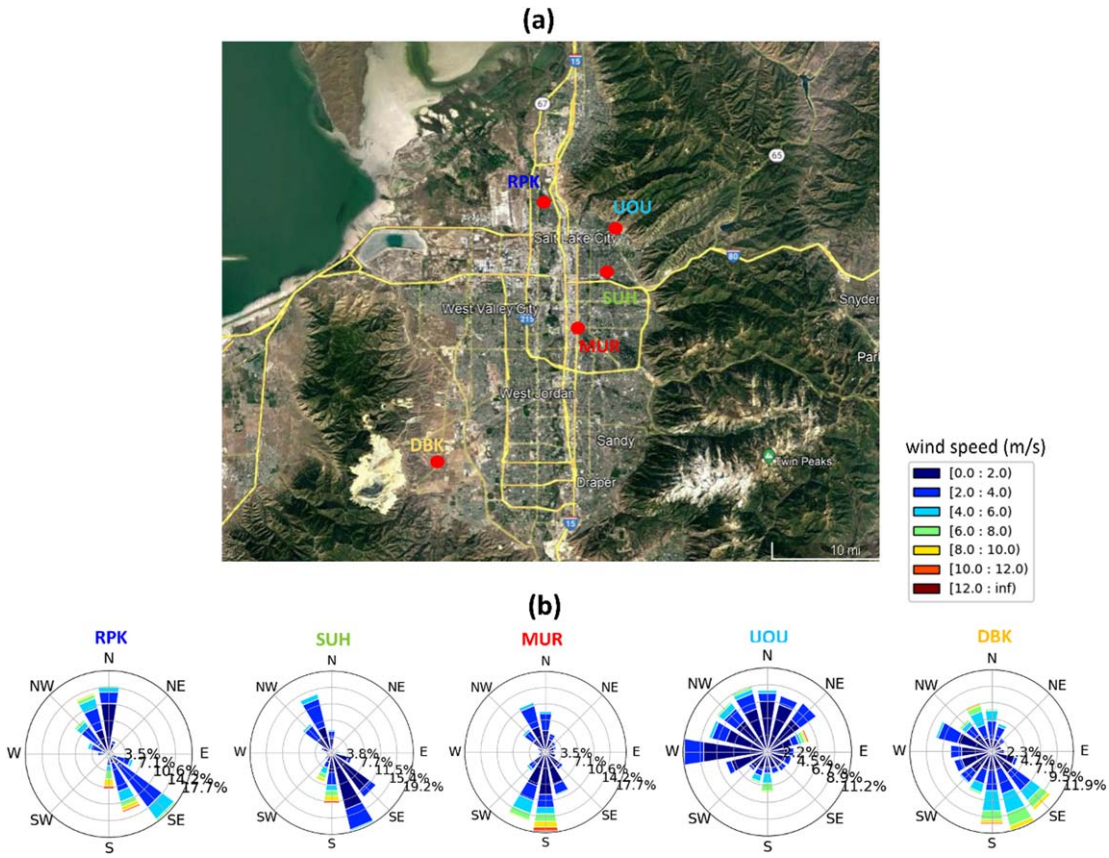

Figure 1. Salt Lake City (SLC) measurement sites and winds: (a) Map of SLC, with red circles marking the observation sites (Rose Park (RPK), Sugar House (SUH), Murray (MUR), University of Utah (UOU), and Daybreak (DBK)). Base map Imagery: Google Earth. Image © Landsat/Copernicus (map downloaded November 17, 2021). (b) Windrose plot for each site during November 2008–2019. The length of the bars within each circle indicates the frequency of wind occurrences [unit in %] in that specific wind direction [degree] and wind speed [m/s] range at a given observation site.

2.2. Vulcan inventory anthropogenic CO_2 flux

The Vulcan3 (Gurney *et al* 2019, 2020) dataset provides hourly, 1 km (~0.01°) gridded data on CO_2 emissions from fossil fuel combustion and cement manufacturing from 10 source sectors in the US for the years 2010 to 2015 (Gurney *et al* 2020). The onroad sector includes CO_2 emissions from most road traffic resources obtained from automobiles, buses, trucks, and motorcycles. The hourly data are obtained by allocating the county/road vehicle-specific CO_2 emissions onto the roadways using the GIS road atlas (NTAD 2003).

Onroad data utilize hourly traffic volume data for the years 2011–2013 obtained from the Federal Highway Administration's Continuous Count Stations (CCS) dataset (previously known as the Automatic Traffic Recorder; ATR) (Gurney *et al* 2020). The CCS stations measure hourly traffic volume at fixed locations, and their latitude and longitude serve as unique station identifiers. To allocate county-scale onroad fossil fuel CO_2 (FFCO2), the fraction of a non-local road class-specific road segment's vehicle miles traveled (VMT) within a county is used as the distribution means. For local roads, due to the scarcity of Annual Average Daily Traffic (AADT) data, the fraction of a road segment's length out of all local roads within a county is employed (Gurney *et al* 2020).

We utilized onroad data to represent traffic-related CO_2 emission sources. Additionally, we derived non-onroad emissions—which include sources such as residential, commercial, and industrial energy use—by subtracting onroad CO_2 emissions from total anthropogenic CO_2 emissions. To identify the dominant emission sector, we analyzed individual sectors like residential, commercial, and industrial as well. Figure 2 presents anthropogenic CO_2 emissions by sector. There is a clear contrast in onroad emissions between weekdays and weekends, with residential emissions being particularly high during the Thanksgiving holidays. Similar patterns are observed in the evening hours (3–7 pm LST). Nonroad and industrial emissions also show similar trends—slightly higher on weekdays than weekends—but their magnitudes are lower compared to the onroad and residential sectors (figure S4). The differences in emissions between weekdays and the Thanksgiving holidays are not very pronounced for these sectors, although there is more variability (larger standard deviation) during the Thanksgiving holidays (figure S4).

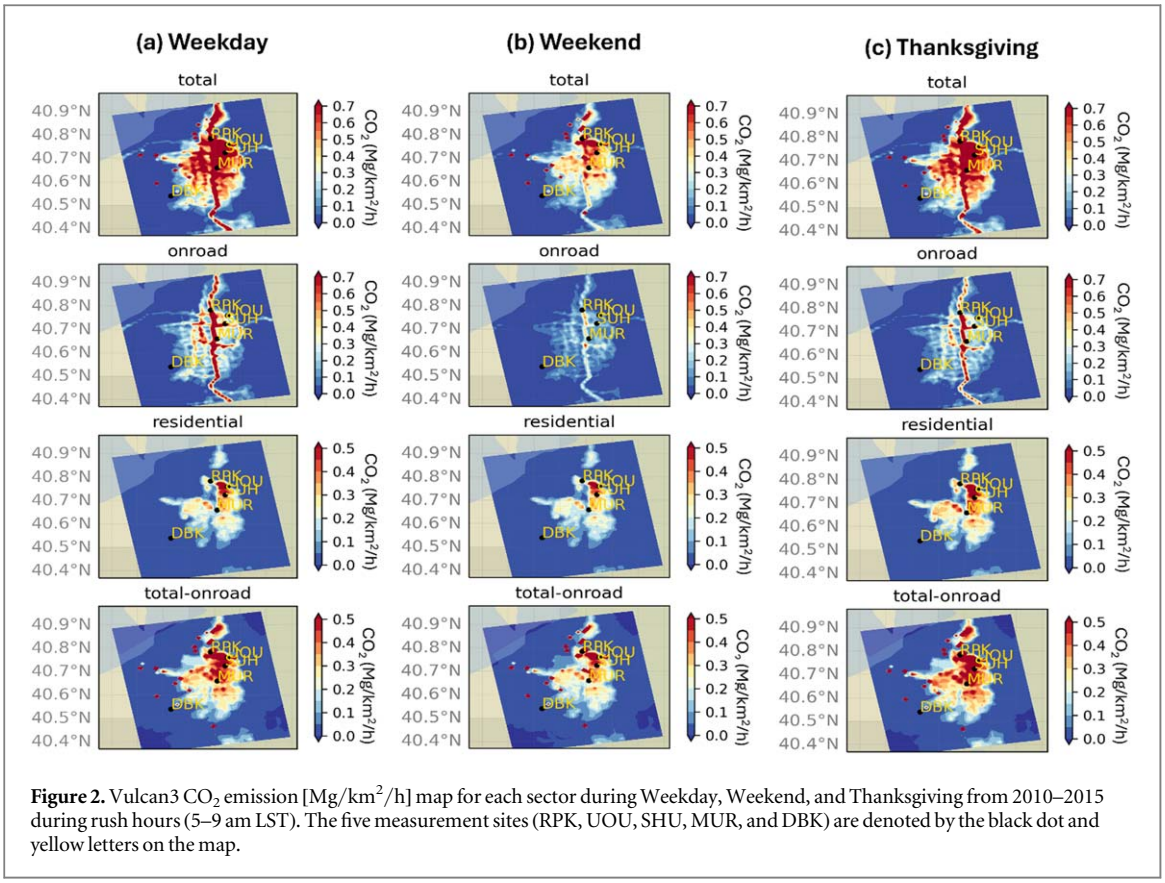

Figure 2. Vulcan3 CO_2 emission [Mg/km^2/h] map for each sector during Weekday, Weekend, and Thanksgiving from 2010–2015 during rush hours (5–9 am LST). The five measurement sites (RPK, UOU, SHU, MUR, and DBK) are denoted by the black dot and yellow letters on the map.

2.3. Random Forest regression and feature importance analysis using SHAP

To assess the factors influencing short-term variations in CO_2 mole fractions, we applied the Random Forest (RF) regressor (Breiman 2001), a supervised ensemble machine learning method well-suited for non-linear regression, obtained from the Python package scikit-learn (Pedregosa *et al* 2011). Our analysis incorporates multiple variables, including meteorological data (e.g., wind speed, wind direction, temperature, relative humidity, and PBLH) and Vulcan3 emission inventories (e.g., onroad and total minus onroad emissions). To assess the contributions of both anthropogenic CO_2 emissions and meteorological factors while mitigating autocorrelation and temporal dependence in time series data, we used data from November 2010–2013 for training and from November 2014–2015 for testing. To assess model performance, we used Pearson's correlation coefficient (R), Root Mean Square Error (RMSE), and Mean Absolute Error (MAE). Additionally, expanding-window time-series cross-validation was employed to ensure robust model validation (figure S10, table S1).

To obtain the fractional feature importance, we employed SHapley Additive exPlanations (SHAP), one of the explainable Artificial Intelligence (XAI) methods (Shapley 1953, Lundberg *et al* 2020, Nelson *et al* 2023), to quantify whether the given feature/factor contributes positively or negatively to CO_2 mole fraction during the different occasions in November over SLC. We used these Vulcan3 emission inventories and meteorological data as 'features' and computed fractional feature importance to understand which features contribute most to CO_2 mole fraction (see the details in figure 9). Positive SHAP values associated with a particular range of feature values indicate that these specific values contribute to an increase in the estimated CO_2 mole fractions output by the RF model. Conversely, negative SHAP values within a given feature's range suggest that these values drive a decrease in the model's CO_2 mole fraction estimations. The relative contribution of each feature is calculated as the ratio of its absolute SHAP value to the sum of absolute SHAP values for all features. The absolute SHAP values are used to capture the magnitude of feature importance, ensuring that contributions are not canceled out by opposing signs. Feature importance was computed using the full November 2010–2015 dataset. Overall, similar patterns are observed across data subsets, though some year-to-year variability exists, particularly during Thanksgiving, partly due to the small dataset size.

3. Results

3.1. The characteristics of observed CO_2 and bottom-up emission sources over SLC

Figure 3 shows the mean diurnal cycle of CO_2 mole fraction (2008–2015) and Vulcan3 emissions (2010–2015) at the five UUCON monitoring sites, averaged over November during weekdays, weekends, and Thanksgiving

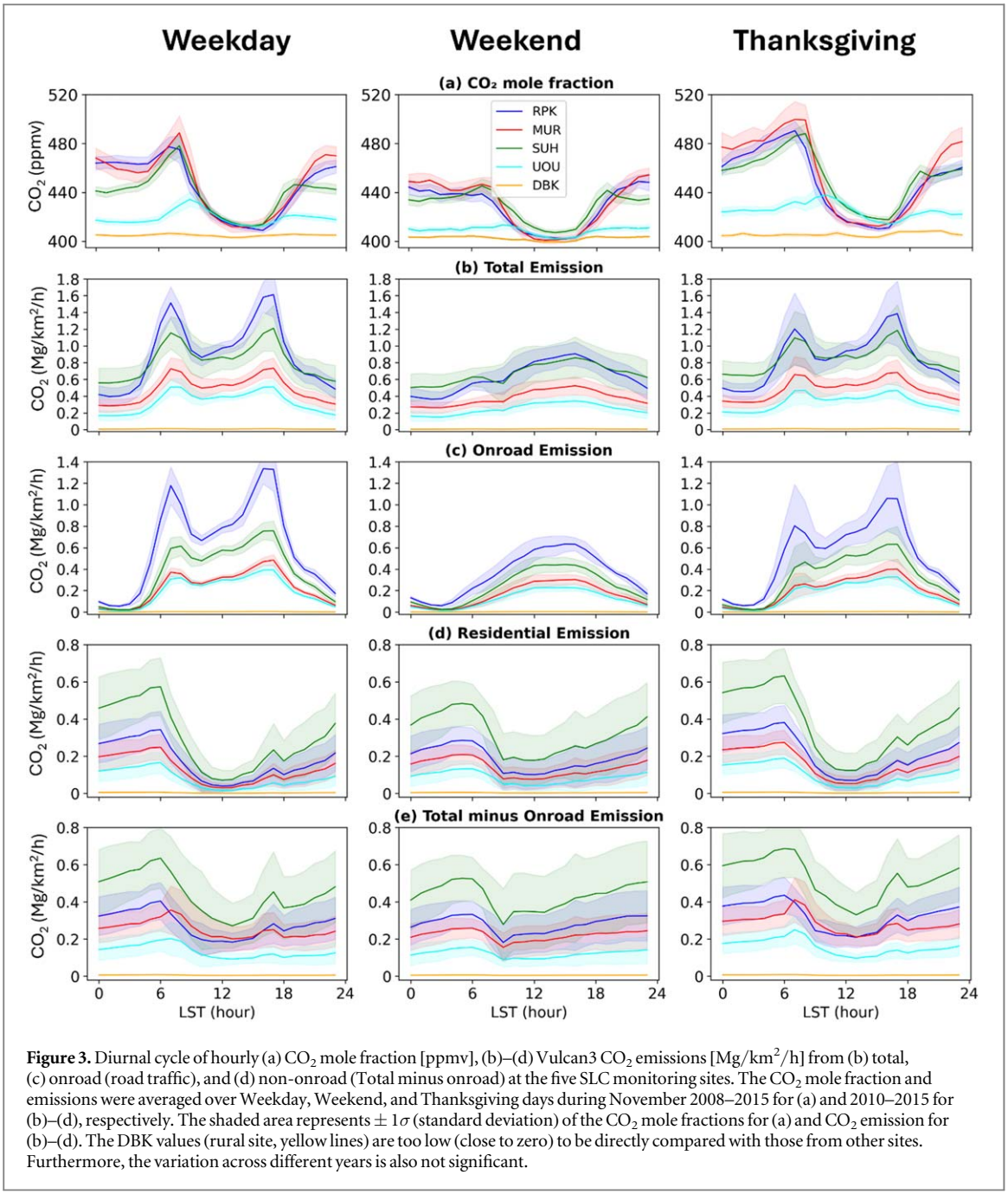

Figure 3. Diurnal cycle of hourly (a) CO_2 mole fraction [ppmv], (b)–(d) Vulcan3 CO_2 emissions [Mg/km^2/h] from (b) total, (c) onroad (road traffic), and (d) non-onroad (Total minus onroad) at the five SLC monitoring sites. The CO_2 mole fraction and emissions were averaged over Weekday, Weekend, and Thanksgiving days during November 2008–2015 for (a) and 2010–2015 for (b)–(d), respectively. The shaded area represents $\pm 1\sigma$ (standard deviation) of the CO_2 mole fractions for (a) and CO_2 emission for (b)–(d). The DBK values (rural site, yellow lines) are too low (close to zero) to be directly compared with those from other sites. Furthermore, the variation across different years is also not significant.

days. As expected for urban sites, CO_2 mole fractions are higher than the ambient CO_2 levels of ~400 ppm and exhibit significant diurnal fluctuations, in contrast to the rural site, DBK. Specifically, CO_2 mole fractions during Thanksgiving surpassed those for weekdays and weekends (figure 3(a)), particularly from 2008 to 2013 at all UUCON sites (figure S1). Similarly, total and non-onroad (total minus onroad) CO_2 emissions, particularly residential CO_2 emissions during Thanksgiving were slightly elevated compared to those during weekdays and weekends, except for the weekday morning rush hour peak (6–8 am, figures 3(a)–(c)), particularly at SUH and RPK with minimal interannual variability (figure S2).

At the rural site, Daybreak, CO_2 emissions show minimal anthropogenic influence (figures 3(b)–(d)). In contrast, urban sites show two onroad CO_2 emission peaks during weekday rush hours, with RPK and SUH exhibiting the highest morning peaks (figure 3(c)), consistent with McKain *et al* (2012). While a lower morning peak is observed during Thanksgiving, non-onroad emissions are generally higher during Thanksgiving than weekdays and weekends, particularly at the primary commercial and residential site SUH, and the near-downtown site RPK, as well as the heavy traffic and industry site MUR (figure 3(d)).

Upon comparing site-by-site CO_2 mole fraction and CO_2 emission, distinct characteristics emerge between emission and mole fraction. For instance, RPK total and onroad CO_2 emissions are higher than SUH and twice as high as MUR during the daytime (7 am–5 pm) (figures 3(b), (c)). However, RPK CO_2 mole fraction is lower

than SUH during the daytime and lower than MUR, especially in the morning and evening. This suggests that other factors may influence the variation in CO_2 mole fractions among sites, which we will explore further in the following section.

3.2. Variations in CO_2 mole fractions across sites: the role of wind advection

In figure 3, higher CO_2 emissions in various residential, commercial, and high-traffic areas, such as RPK, SUH, and MUR are evident relative to the lower-traffic areas of UOU and DPK. The anthropogenic CO_2 mole fraction closely correlates with these increased emissions, as indicated by the elevated CO_2 mole fraction in RPK and SUH shown in figure 3(a). However, emissions alone do not fully account for the overall variation in CO_2 mole fraction. For instance, CO_2 mole fractions are higher in Murray (MUR) than in RPK, despite MUR's CO_2 emissions being only half of those in RPK (figure 3(a)). These divergent results suggest that additional factors contribute to the differing behaviors in CO_2 mole fraction observed during different occasions in November, such as biological processes, entrainment, or meteorological controls.

Biological processes are typically less active in urban areas during the cool seasons due to limited green space (Strong *et al* 2011). To assess the potential contribution of biological flux, we initially utilized 3-hourly, Carbon Tracker 2019B data (CT; Jacobson *et al* 2020). However, no significant differences in biological flux were observed among times (not shown). We acknowledge that this is partially due to the coarse resolution of the data, but biological CO_2 flux is relatively small during this time of year, even when using higher-resolution data (e.g., Strong *et al* 2011, Mallia *et al* 2023). Furthermore, considering the response time of vegetation to environmental controls, short-term CO_2 variations may not be fully explained by biological flux. Entrainment serves as a significant CO_2 sink during the morning and early daytime (Strong *et al* 2011) and is highly influenced by the PBLH, making PBLH a key indicator of CO_2 variation. However, entrainment alone cannot fully account for the observed CO_2 variations for most of daytime and evening hours (Strong *et al* 2011). Therefore, we analyzed the role of regional PBLH in CO_2 variation by estimating it across different occasions (weekdays, weekends, and Thanksgiving), as discussed in section 3.

Meteorological factors, such as wind-driven advection of emissions and other anthropogenic sources, are also important to consider. We hypothesized that onroad CO_2 emissions would be advected with southerly and northerly winds, given the proximity of the MUR and SUH sites to major highways (figure 1(a)). To explore the influence of wind advection on CO_2 mole fractions between sites, we conducted a more comprehensive analysis, as shown in figure 4.

To investigate the factors contributing to the discrepancy in patterns between high CO_2 mole fraction and high CO_2 emissions, we initially focus on regions with high emission sources, including residential, heavy-traffic, and commercial sites—RPK, MUR, and SUH—where the most significant differences in CO_2 emission and CO_2 mole fraction are observed (figure 3), with wind patterns.

Figure 4 illustrates that when the wind direction at MUR is southerly (around 180 degrees) and slightly northerly (near 0 and 360 degrees) (figure 4(c)), aligning with the north-south-oriented highway, the CO_2 mole fraction at RPK and MUR starts to converge (figure 4(a)). This suggests the advection of CO_2-rich air from the highway toward MUR (figure 2). Consequently, the CO_2 mole fraction at MUR can exceed that at RPK, despite MUR having lower emissions (figure 4(a)). More distinct results were shown when comparing SUH, the second largest non-onroad emission site, with RPK. For instance, SUH's CO_2 mole fraction was notably higher by up to 100 ppmv than RPK when the wind blew from the south (around 180 degrees) and northwest (around 330 degrees) (figures 4(b), (d)), especially on weekdays and weekends when winds are relatively high. The wind patterns at RPK are quite similar to those at SUH, with more northerly winds observed during weekdays and weekends. However, much lower winds were observed at RPK during Thanksgiving compared to SUH (not shown).

Our observation of higher CO_2 levels from the heavy-traffic regions aligns with the findings from atmospheric inversion modeling presented in Mallia *et al* (2023). In contrast, SUH's CO_2 mole fractions get lower than RPK when the wind originates from the northeast (around 60 degrees), from a cleaner rural mountain region, across all weekdays, weekends, and Thanksgiving (figures 4(b), (d)). These findings underscore 1) the significant role of traffic and wind advection in contributing to high CO_2 mole fractions, and 2) multi-site observation points are needed to understand spatial patterns of emissions using atmospheric data. Such insights should be considered when planning CO_2 observation networks.

3.3. CO_2 variability under different meteorological conditions: a comparison between November 2008–2013 and 2014–2019

Interestingly, there is a notable contrast in the CO_2 mole fraction during the Thanksgiving holidays between most of the periods of 2008–2013 (Period I) and 2014–2019 (Period II) over the five measurement sites in the SLC. Elevated CO_2 levels during Thanksgiving were only observed mostly in Period I in SLC (figure S1). To

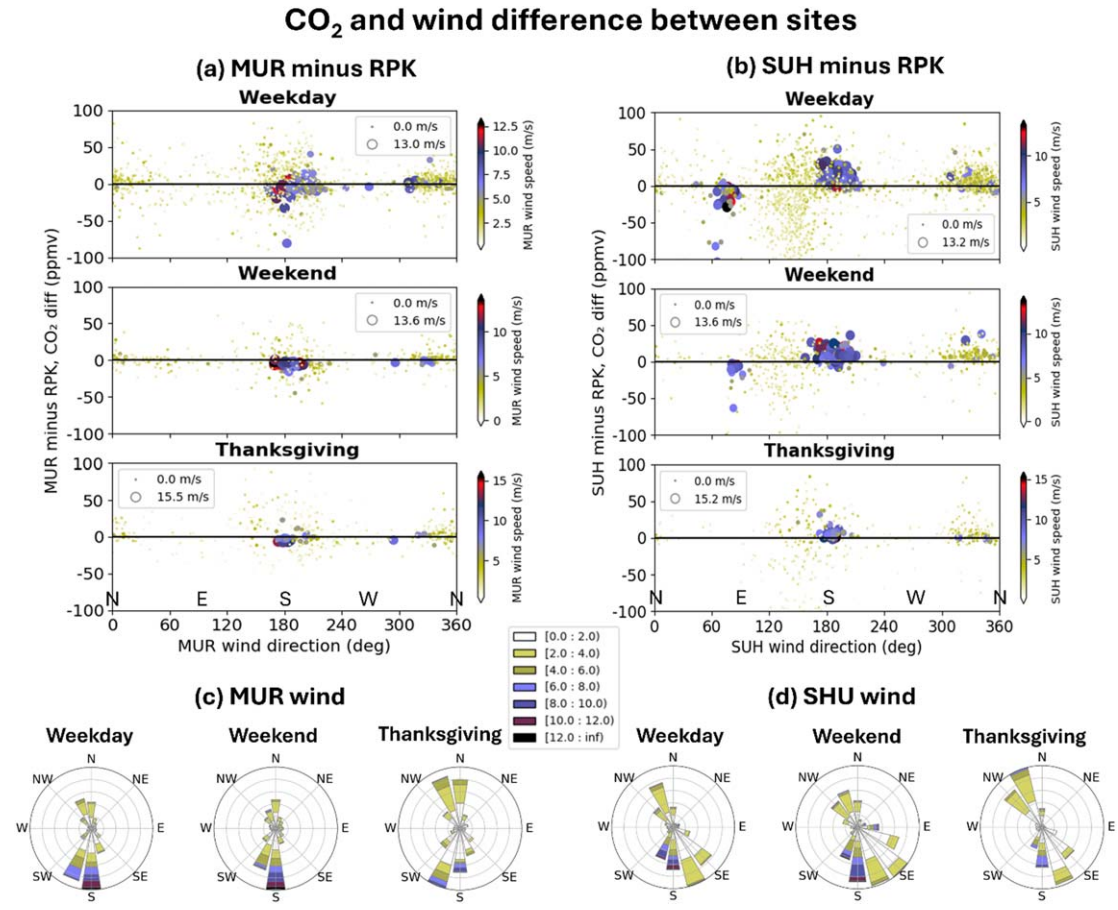

Figure 4. (a) Scatter plots illustrating the difference in CO_2 mole fraction [ppmv] from Murray (MUR) to Rose Park (RPK) relative to the MUR wind direction [degree] during (top) Weekday, (middle) Weekend, and (bottom) Thanksgiving from 2009–2012. (b) The same as (a) except for from Sugar House (SUH) to RPK relative to the SUH wind direction from 2009–2015. The marker color and size represent the wind speed [m/s] at each site, while N, E, S, and W indicate the wind direction—north, east, south, and west, respectively. (c), (d) Windrose plots at MUR (2009–2012) and SHU (2009–2015) depict wind speed and direction on different occasions (Weekday, Weekend, and Thanksgiving).

understand what drives this difference, we observed the yearly difference in emissions by sector, shown in figure 5. There is weak yearly variability across all emission sectors, with a distinct increase observed in 2013. Daily average emissions for the onroad sector are higher on weekdays compared to weekends and Thanksgiving for all years. Industrial and nonroad emissions were small ($<0.05\ Mg\ km^{-2}\ h^{-1}$), but they are all higher during weekday (figure S5). In contrast, emissions from the residential sector and all non-onroad sources (total emissions minus onroad) are higher during Thanksgiving each year (figures 5(c), (d)), especially in 2013. Thanksgiving emissions were relatively similar between 2010–2013 and 2014–2015, with even lower weekday and weekend emissions in 2014–2015. We will further examine the role of meteorology in influencing these distinct patterns of short-term CO_2 variability.

We examined the meteorological factors influencing CO_2 changes, as shown in figure 6. During Thanksgiving in Period I (2008–2013), conditions were mostly drier, cooler, and weaker surface winds compared to the rest of November in Period II (2014–2019). A negative relationship between CO_2 mole fraction and both temperature and surface wind speed was observed (figure 6). For example, during the 2013 Thanksgiving holiday, CO_2 mole fraction was highest when temperatures were coldest (figures 6(a), (c)), surface winds were weakest (figures 6(a), (b), figures 7(a), (c)). These combined effects likely contributed to the observed increase in CO_2 mole fractions during Thanksgiving in Period I. CO_2 mole fraction also tends to decrease with increasing PBLH, a pattern clearly observed during Thanksgiving and the years 2014–2019 (figure 7). PBLH tends to be low during the Thanksgiving holidays from 2008 to 2013 compared to most years of 2014–2019, especially 2016 (figures 7(b), (d), S6).

A negative relationship between CO_2 mole fraction and daily mean temperature during different occasions (weekdays, weekends, and Thanksgiving) was also observed, but it was not as strong as the one between CO_2 mole fraction and surface wind speed (not shown). We hypothesize that this might be due to the diurnal

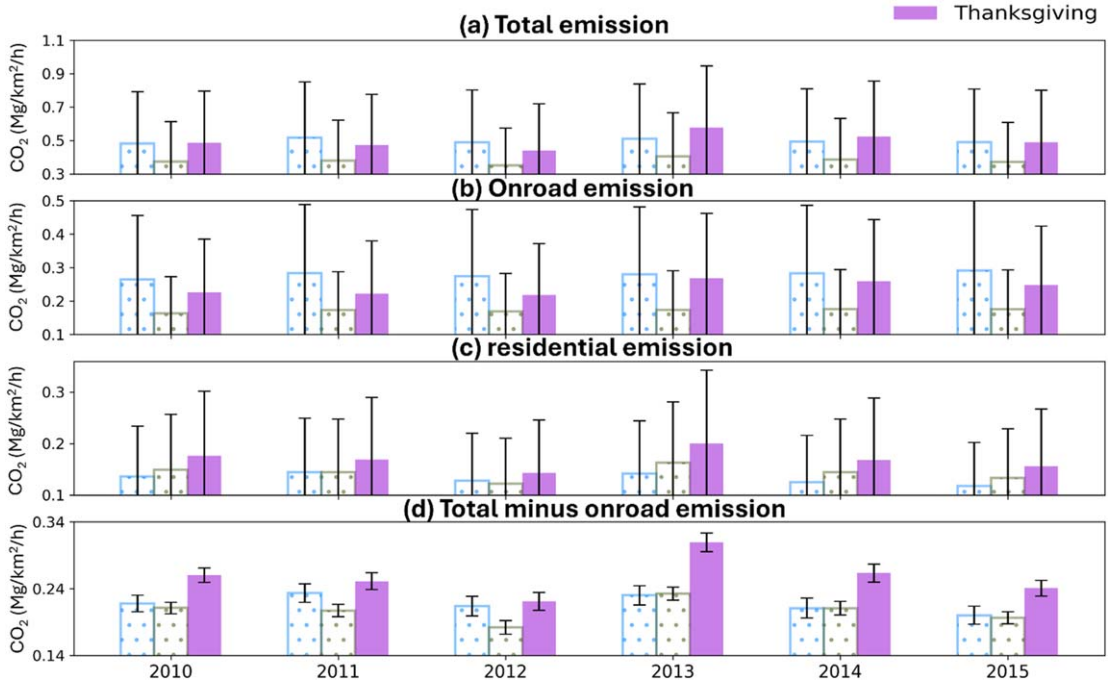

Figure 5. Vulcan3 emissions [Mg/km^2/h] from (a) Total, (b) onroad, (c) residential, and (d) total minus onroad from 2010 to 2015 during Weekday, Weekend, and Thanksgiving days averaged over the closest point to the five CO_2 measurement sites in SLC marked on figure 2. The error bar represents the $\pm 1\sigma$ from the five measurement sites for each year.

variation in temperature and its impact on CO_2 variability. To explore this relationship further, we analyzed CO_2 and temperature separately for day and night, as depicted in figure 8.

Hourly CO_2 mole fractions were averaged across five sites for each Period. Weekdays and weekends CO_2 were higher in Period II than Period I, and CO_2 mole fractions were lower during daylight hours (7 am–5 pm) than nighttime (figures 8(a), (b)). Thanksgiving CO_2 shows a different variation. Thanksgiving daytime CO_2 was approximately the same between the two periods, while nighttime increase was more pronounced in Period I than Period II. (figure 8(a)). Nighttime temperatures were lower during Thanksgiving during Period I and likely contributed to increased residential energy consumption and higher CO_2 (figures 3(d), 8(c)). Previous studies showed that heating degree days are strongly linked to energy use (Petrick *et al* 2010, Mourshed 2012, Li *et al* 2021, Yadav *et al* 2021). Petrick *et al* (2010) support the association between colder temperatures and greater residential energy use. Li *et al* (2021) also reported elevated electricity consumption in urban regions during colder days. This is also reflected in our analysis using Vulcan CO_2 emission, particularly in the cold days during Thanksgiving in 2010 and 2013. Although there is no significant interannual variability in CO_2 emissions for onroad sources, we observe a clear increase in residential emissions over urban residential areas such as SUH and RPK on Thanksgiving than on weekdays and weekends (figures 5(c), (d), S3).

Our analysis revealed a significant increase in CO_2 levels on weekdays, more than double those observed on Thanksgiving, when controlling temperature effects (figure S8). This finding warrants further investigation, as traffic and human activity are likely important contributing factors. Although the relationship between temperature and CO_2 is complex, temperature is a key climate driver influencing CO_2 variation. Our results indicate that changes in residential heating, energy use, and meteorological conditions contribute to CO_2 variation (figure S7) (Parazoo *et al* 2008, Newman *et al* 2013, Xueref-Remy *et al* 2018, Agustí-Panareda *et al* 2019). This supports that temperature can serve as a reliable indicator of energy use and CO_2 emissions in urban areas.

3.4. Contributing factor analysis

In the previous section, we analyzed meteorological conditions and anthropogenic emissions over SLC, leading to an important question: What primarily drives the observed CO_2 mole fractions? As observed, CO_2 variability is governed by highly nonlinear variables, referred to here as 'features,' including meteorological factors and the type and magnitude of emissions. To disentangle these effects, we conducted an RF-based SHAP analysis in figure 9. In SHAP analysis, a feature's contribution increases when it has a high value—either positively or

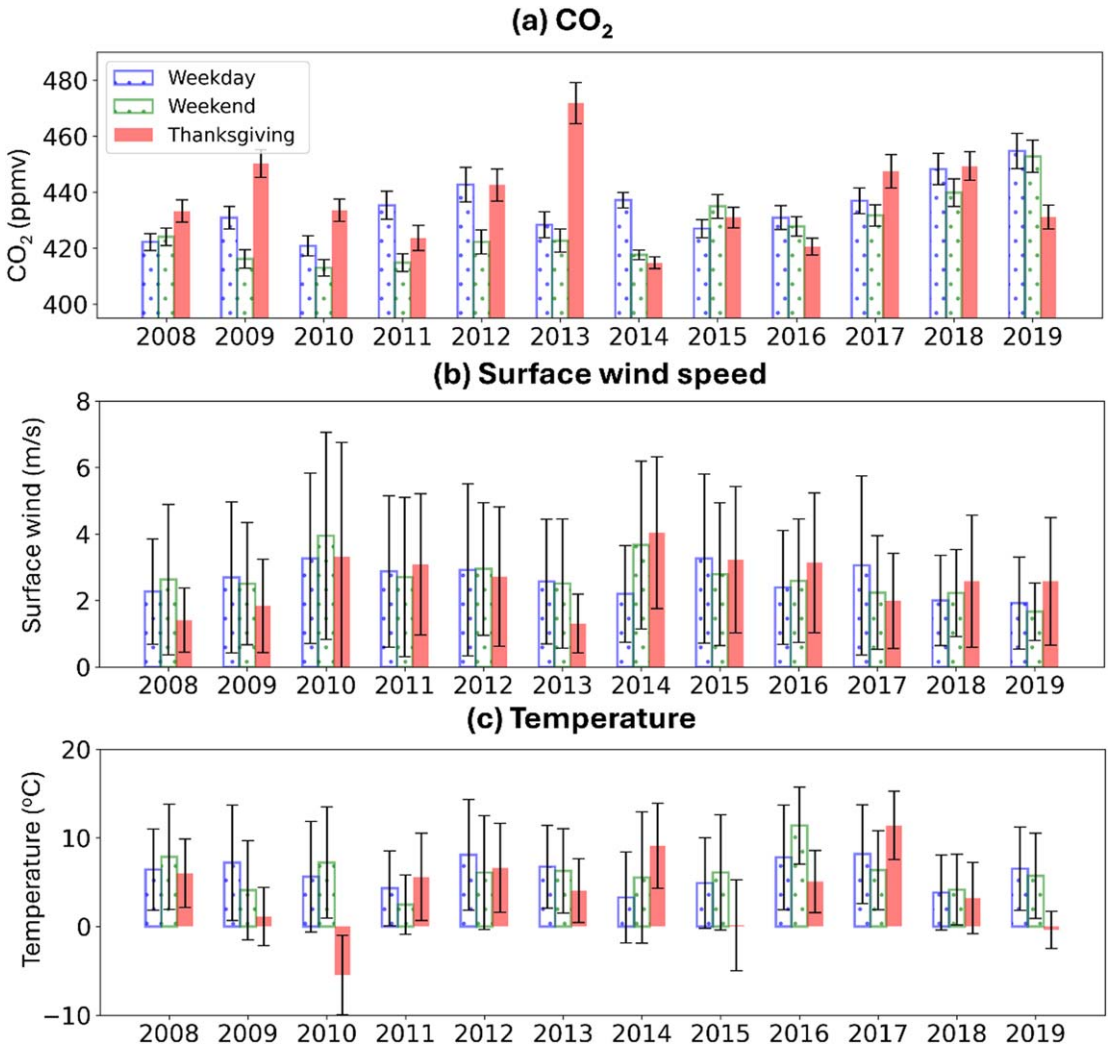

Figure 6. Bar plots of the mean (a) CO_2 mole fraction [ppmv], (b) surface wind speed [m/s], and (c) temperature [°C) averaged over the five CO_2 measurement sites over SLC during Weekday, Weekend, and Thanksgiving. The error bar represents the $\pm 1\sigma$ from the five measurement sites for each year.

negatively—on CO_2 mole fractions over SLC during weekdays, weekends, and Thanksgiving in November from 2010 to 2015. The RF model effectively captures the overall patterns of CO_2 mole fractions (figure S10) and performs reasonably well (table S1).

Over the study period, three key findings emerge from figure 9. *First*, meteorological factors dominate CO_2 modulation. SHAP analysis indicates that wind speed and PBLH play a dominant role in modulating CO_2 mole fractions across all occasions (figures 9(a)–(c)), contributing up to ~45% and ~25% of the variability, respectively, depending on the specific occasion. This is likely due to enhanced dispersion and pollution transport under high wind conditions (Vasumathi *et al* 2017), as supported by figure 4. This aligns with Xueref-Remy *et al* (2018), who demonstrated the high sensitivity of *in situ* CO_2 measurements in the Paris megacity region to wind speed, wind direction, and PBLH. *Second*, while meteorological variables consistently influence CO_2 levels, their relative importance varies by occasion. For instance, onroad emissions contribute more on weekdays than weekends, reflecting traffic patterns. During Thanksgiving, energy-related emissions (total minus onroad, referred to as the 'energy' sector) become the dominant source. The relative impact of energy emissions during Thanksgiving varies by year. For example, from 2010 to 2015, the overall contribution was approximately 5%, while in 2014, it was estimated up to ~12% (figure S11). In contrast, contributions during weekdays (~4%) and weekends (~3%) remained consistent (figures 9, S11). *Third*, complex interactions are found between factors (features) to drive CO_2 variation. Multiple factors influence CO_2 in different, sometimes opposing ways. For instance, onroad emissions increase CO_2 under low wind speeds and a shallow PBLH but may have a diminishing effect under high wind speeds, depending on wind direction (e.g., pollution transport, as shown in figure 4). As highlighted by the SHAP analysis (figure 9(c)), non-onroad energy emissions contribute

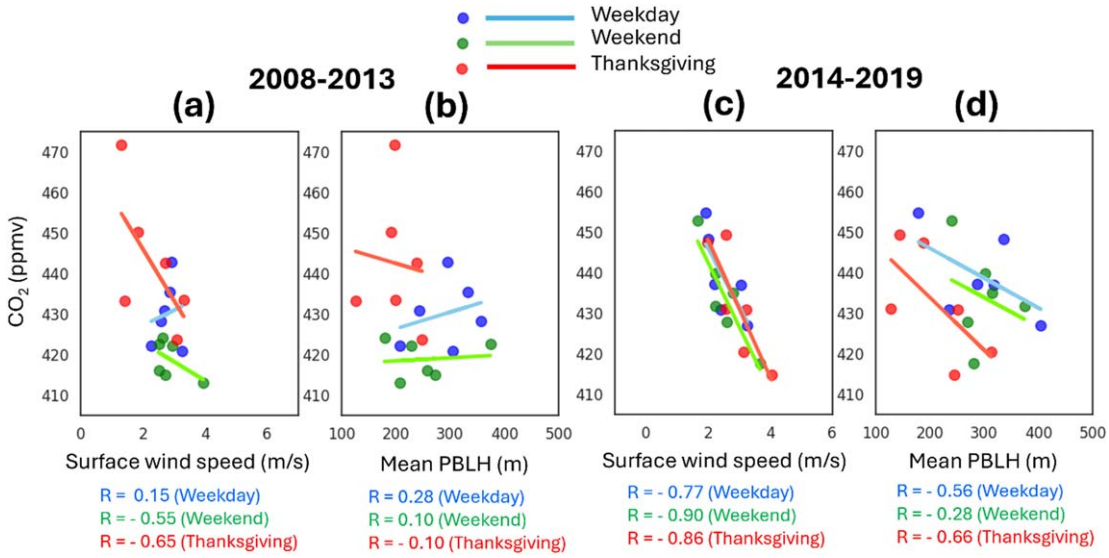

Figure 7. Relationship between CO_2 mole fraction [ppmv] and (a, c) surface wind speed [m/s] averaged over five CO_2 measurement sites in SLC, and (b, d) CO_2 mole fraction and mean PBLH [m] for different occasions (Weekday (blue), Weekend (green), and Thanksgiving days (red)) for (left) Period I (2008–2013) and (right) Period II (2014–2019). Each color dot represents values averaged by occasion and by each November of each year. The color line represents the regression of the values for each occasion and each period, respectively. R represents Pearson's correlation coefficient during each occasion, respectively.

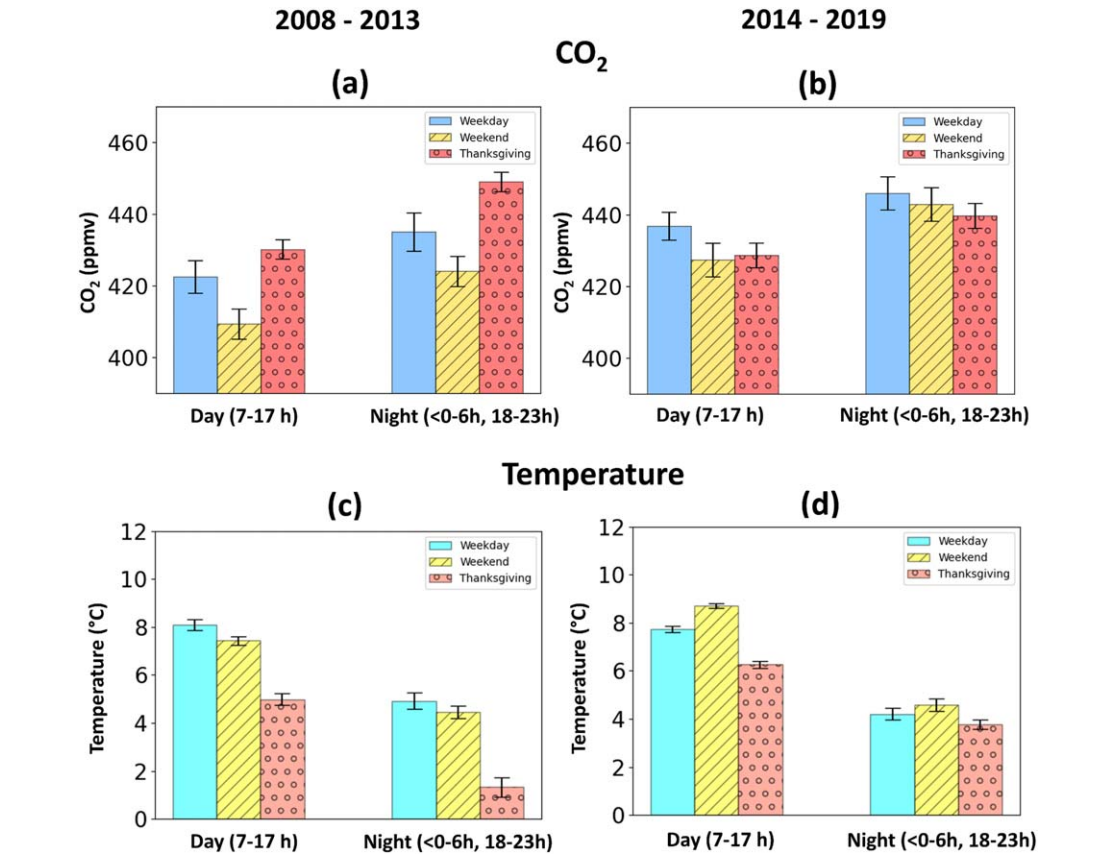

Figure 8. Diurnal difference in (a, b) CO_2 [ppmv] and (c, d) temperature [°C] during different periods. The daytime (7–17h; left) and the nighttime (0–6h, 18–23h; right) CO_2 mole fractions during Weekday (blue), Weekend (yellow), and Thanksgiving (green). The error bar represents $\pm 1\sigma$ of the CO_2 mole fractions for different periods (Period I: 2008–2013 and Period II: 2014–2019, respectively).

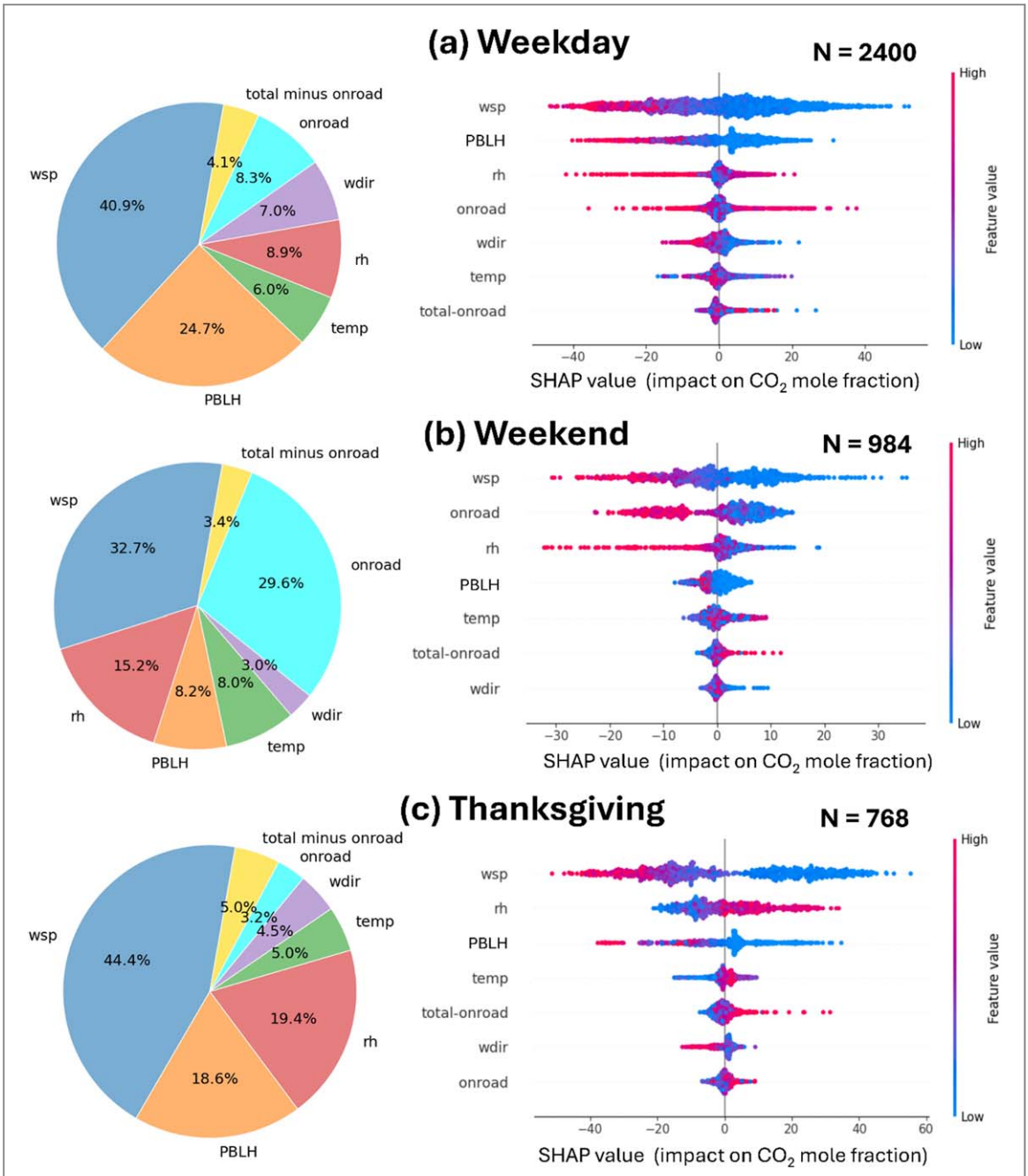

Figure 9. Feature importance of SLC CO_2 mole fraction: (Left) RF- SHAP-based fractional factor contributions, and (Right) RF-SHAP values of CO_2 mole fraction averaged over five CO_2 measurement sites for its features such as meteorological variables (wind speed (wsp), wind direction (wdir), temperature (temp), PBLH, relative humidity (rh)), and Vulcan3 emission data (onroad, total-onroad) during (a) Weekday, (b) Weekend, and (c) Thanksgiving in November 2010–2015.

more positively to CO_2 increases under low temperatures (figure S10), aligning with the patterns observed in figures 5 and 6.

Note that the factors used in this study can vary depending on geographical regions and seasons. For example, the impact of biological emissions on CO_2 is minimal during the cool season, so we did not include them in our analysis. However, they can be a key driver of CO_2 variability in the warm season and should be considered as an important factor. Furthermore, the loss of saline lakes under drought conditions can be a significant source of increased CO_2 in arid regions like SLC and is expected to worsen with climate change (Cobo *et al* 2024), as suggested by relative humidity (rh, figure 9) in our analysis. Although its impact remains relatively small during cool seasons like November (Cobo *et al* 2024), its influence on CO_2 variability across other seasons warrants further investigation. Improved understanding of the dominant factors controlling CO_2 variation—and how they change over time and across regions at the urban scale—will support effective emission mitigation planning.

4. Discussion

CO_2 mole fractions are influenced by both meteorological conditions and emissions, which vary by sector, occasion, and period, as observed in SLC. In the previous section, short-term fluctuations in emission types were identified across different timeframes—weekdays, weekends, and Thanksgiving. For example, energy-related emissions (total minus onroad) were higher during Thanksgiving, whereas onroad emissions peaked on weekdays. Beyond these temporal variations, meteorological and geographic factors further shape CO_2 mole fraction behavior across cities due to differences in climate, topography, and industrial activity. As a result, CO_2 mole fractions in cities like San Francisco (SF) and Boston differed from those in SLC (not shown).

To examine emission types independent of geographical and meteorological conditions, we analyzed emissions across multiple locations and identified consistent characteristics (figure 10). In major metropolitan areas such as Boston and Los Angeles (LA), total CO_2 emissions were more than twice as high as in smaller cities like SLC and Portland (PL) (figure 10(a)). Onroad emissions remained consistently high on weekdays across all cities, with minimal year-to-year variation (figure 10(b)). In contrast, residential and commercial emissions were higher during Thanksgiving than on weekdays and weekends, especially in large urban areas like Boston and LA, exhibiting significant year-to-year variability, likely influenced by local temperature fluctuations (Petrick *et al* 2010) (figures 10(c), (d)). Overall, energy-related emissions (total minus onroad, including residential and commercial sectors) exhibited substantial year-to-year variability, with peaks occurring during Thanksgiving (figure 10(e), S9).

The emission data correspond to the urban sites closest to each CO_2 measurement location, as listed in table S2.

5. Conclusions

To gain a deeper understanding of the factors driving the short-term CO_2 variations across monitoring sites in Salt Lake City (SLC), we conducted a multi-year analysis of high-frequency CO_2 mole fraction observation, Vulcan3 anthropogenic CO_2 emission, as well as the meteorological data on weekdays, weekends, and Thanksgiving from 2008 to 2019 (with subset of 2010–2015 for accounting for anthropogenic CO_2 emission impact). The main findings and novelty of this study are summarized below.

- **Elevated CO_2 mole fractions are observed during Thanksgiving in 2008–2013 over SLC**. This is closely associated with the short-term energy use change (e.g., increases in residential and commercial emissions) and meteorological conditions such as cold temperature, weak surface wind, and low planetary boundary layer height (PBLH), contrasting to the years 2014–2019.
- **The Vulcan version 3 (Vulcan3) onroad CO_2 emission fluxes exhibited two peaks of traffic-related CO_2 fluxes during weekdays over SLC**, indicating the increase of CO_2 emissions during the morning and evening rush hours. Non-road anthropogenic CO_2 emissions, including those from industrial, commercial, residential energy consumption, and other non-road sources, were up to 33% higher (~0.1–0.2 Mg km^{-2} h^{-1}) during Thanksgiving compared to weekdays and weekends.
- The high CO_2 mole fraction over Murray (MUR) and Sugar House (SUH), despite its relatively low CO_2 emission, is primarily due to southerly and weak northwesterly wind advection. **This highlights the significance of strategic planning for multi-site measurements to precisely identify emission sources**.
- **Random Forest (RF)-based SHapley Additive exPlanations (SHAP) feature importance analysis highlights the key role of meteorological factors—**including wind speed, PBLH, relative humidity, and temperature—in modulating CO_2 variability. Short-term variations in onroad emissions influence CO_2 levels during weekdays and weekends. Conversely, energy sector emissions are notable contributors to CO_2 levels during Thanksgiving in SLC.
- **This elevated emission pattern during Thanksgiving was observed not only over SLC but also across other urban cities**, such as Boston, Washington D.C., Los Angeles, San Francisco, and Portland.

While this study demonstrates that short-term CO_2 variations are influenced by both emissions and meteorology, further research is needed. *First,* our analysis utilizes Vulcan3 emission data to assess sector-based traffic and energy use changes. While this high-resolution hourly dataset is valuable for identifying short-term CO_2 variability, it is only available from 2010 to 2015, which may limit its ability to capture traffic variations over the full study period. *Second,* we found that emission patterns during Thanksgiving were consistent across six urban cities. However, given the combined influence of emissions and meteorological conditions on CO_2 levels,

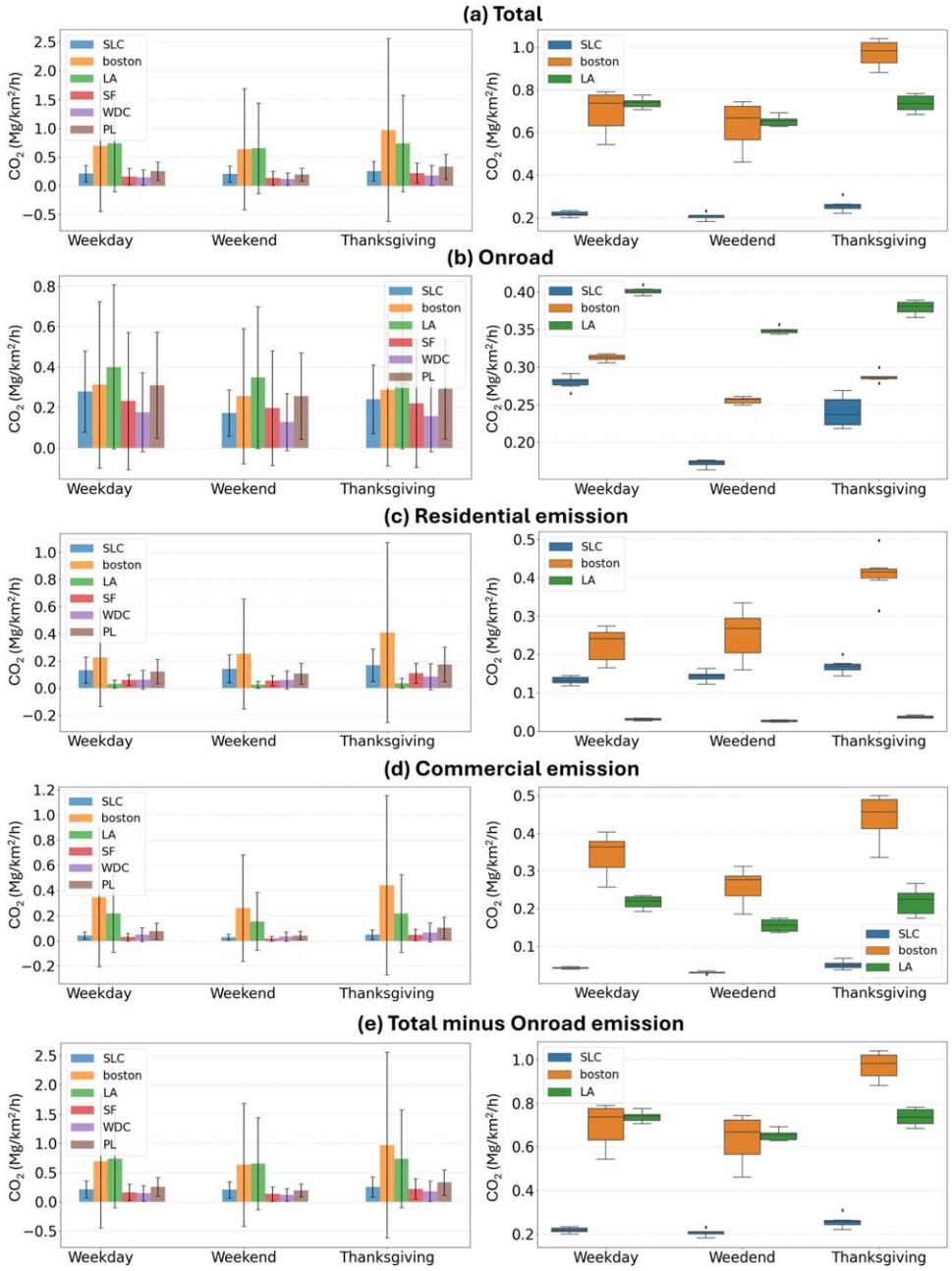

Figure 10. Vulcan3 CO_2 emissions [Mg/km^2/h] by sector across urban cities: (Left) bar plots of (a) total, (b) onroad, (c) residential, (d) commercial, and energy (total minus onroad) emissions for six cities (SLC, Boston, Los Angeles (LA), San Francisco (SF), Washington D.C. (WDC), Portland (PL)). The vertical bar represents $\pm 1\sigma$ of CO_2 emissions from 2010 to 2015 for each city. (Right) Box plots of total, onroad, residential, commercial, and energy emissions for three urban cities (SLC, Boston, LA) in November 2010–2015.

expanding this study to other regions and seasons would be a valuable research opportunity. Future studies can leverage advancements in remote sensing (e.g., Orbiting Carbon Observatory-2 and -3 (OCO-2 and OCO-3)) and regional modeling, integrating *in situ* measurements for improved analysis. *Third*, high temporal and spatial resolution measurements will enhance our understanding of the factors controlling CO_2 variation. For example, improved hourly measurements—such as winds and PBLH, particularly during nighttime at multiple measurement sites—will enhance the estimation of hourly CO_2 variations over cities.

Hutyra *et al* (2014) emphasized the importance of understanding emission sources, their variability, and the controlling processes of urban carbon fluxes—essential for advancing carbon cycle science and informing effective emission reduction policies. Urban CO_2 enhancements are not in steady state, as fossil fuel emissions respond dynamically to changes in human behavior (Hutyra *et al* 2014). Our findings demonstrate that both meteorology and human-driven energy use contribute to short-term CO_2 variability at the city scale (Newman *et al* 2013, Xueref-Remy *et al* 2018), occurring consistently rather than as isolated events and likely to evolve further under a warming climate (Cobo *et al* 2024). These findings emphasize the critical need for sustained CO_2

monitoring, enhanced meteorological data acquisition, optimized monitoring site selection, reinforced onroad vehicle emission regulations, and a practical, comprehensive observational-modeling framework to refine source attribution and emission reduction strategies across various urban environments.

Acknowledgments

This work is supported by the Department of Energy under Award Numbers DE-FG02-07ER64436 and DE-SC0006625 and by NSF Awards EF-01241286 and EF-01240142. Resources supporting this work were provided by the National Energy Research Scientific Computing Center (NERSC) at UC Berkeley and NASA High-End Computing (HEC) Program through the NASA Advanced Supercomputing (NAS) Division at NASA Ames Research Center. We also acknowledge NASA Award 80NSSC23M0230. We thank Dr John C. Lin for his support in data acquisition. We also extend our appreciation to Dr Logan Mitchell for his assistance with data acquisition and scientific comments. Finally, we thank the editor and anonymous reviewers for their helpful comments.

Author contributions

J.-M. Ryoo: Conceptualization, Data curation, Formal analysis, Investigation, Methodology, Writing - original draft, review & editing, Visualization; I. Fung: Conceptualization, Formal analysis, Investigation, Methodology, Writing, review & editing, Visualization, Funding acquisition, Resources, Supervision; J. Ehleringer: Resources, Writing—review & editing.

Declaration of competing interest

The authors declare no competing financial interests or personal relationships exist.

Data availability

The surface *in situ* Salt Lake City (SLC) CO_2 mole fraction data are available from https://daac.ornl.gov/cgi-bin/dsviewer.pl?ds_id=1916. The Vulcan Version 3 (Vulcan3) High-Resolution hourly Fossil Fuel CO_2 Emissions in the USA dataset in 2010–2015 are obtained from https://doi.org/10.3334/ORNLDAAC/1741. The meteorological data on wind and surface temperature over the SLC sites are obtained from the MesoWest sites (http://mesowest.utah.edu/). The hourly surface temperature data at Salt Lake City International Airport are available from Weather Underground (https://www.wunderground.com/history/daily/KSLC/date) and atmospheric sounding data (SLC, #72572) are available from the University of Wyoming Atmospheric Sounding Site http://weather.uwyo.edu/upperair/sounding.html. The hourly ERA 5 meteorological reanalysis data are available from the Copernicus Climate Change Service (C3S) https://cds.climate.copernicus.eu/cdsapp#!/dataset/reanalysis-era5-pressure-levels?tab=overview.

ORCID iDs

Ju-Mee Ryoo https://orcid.org/0000-0002-3425-6296
Inez Fung https://orcid.org/0000-0003-4106-9875
James R Ehleringer https://orcid.org/0000-0003-2050-3636

References

Agustí-Panareda A *et al* 2019 Modelling CO_2 weather—why horizontal resolution matters *Atmos. Chem. Phys.* **19** 7347–76
Apadula F, Gottia A, Piginia A, Longhettob A, Rocchettia F, Cassardob C, Ferrareseb S and Forzab R 2003 Localization of source and sink regions of carbon dioxide through the method of the synoptic air trajectory statistic *Atmos. Environ.* **37** 3757–70
Bares R, Mitchell L, Fasoli L, Bowling B, Catharine D R, Garcia D, Eng M, Ehleringer B, Lin J and C J 2019 The Utah urban carbon dioxide (UUCON) and Uintah Basin greenhouse gas networks: instrumentation, data, and measurement uncertainty *Earth Syst. Sci. Data* **11** 1291–308
Barth M and Boriboonsomsin K 2008 Real-world carbon dioxide impacts of traffic congestion *Transp. Res. Rec.* **2058** 163–171
Breiman L 2001 Random forests *Mach. Learn.* **45** 5–32
Cobo M, Goldhammer T and Brothers S 2024 A desiccating saline lake bed is a significant source of anthropogenic greenhouse gas emissions *One Earth* **7** 1414–23
Day T A, Gober P, Xiong F S and Wentz E A 2002 Temporal patterns in near-surface CO_2 concentrations over contrasting vegetation types in the Phoenix metropolitan area *Agric. For. Meteorol.* **110** 229–45

Ehleringer J, Moyes A, Cook C, Pataki D E, Lai C -T and Schauer A 2009 Long-term results from an urban CO_2 monitoring network *Eos Trans.* (AGU) Fall Meet. Suppl., Abstract B33D-0414
Ehleringer J, Schauer A J, Lai C -T, Bowling D R, Pataki D E and Stephens B B 2008 Long-term carbon dioxide monitoring in Salt Lake City *Eos Trans.* (AGU) Fall Meet. Suppl., Abstract B43D-0466
Gratani L and Varone L 2005 Daily and seasonal variation of CO_2 in the city of Rome in relationship with the traffic volume *Atmos. Environ.* **39** 2619–24
Gualtieri G, Lonardo S D, Carotenuto F, Toscano P, Vagnoli C, Zaldei A and Gioli B 2021 The role of emissions and meteorology in driving CO_2 concentrations in urban areas *Environmental Science and Pollution Research* **28** 29908–18
Gurney K R *et al* 2015 Tracking urban emissions on a human scale *Nature* **525** 179–81
Gurney K R, Liang J, Patarasuk R, Song Y, Huang J and Roest G 2019 *Vulcan: High-Resolution Annual Fossil Fuel CO_2 Emissions in USA* (ORNL DAAC) 2010–5 Version 3
Gurney K R, Liang J, Patarasuk R, Song Y, Huang J and Roest G 2020 The Vulcan version 3.0 high-resolution fossil fuel CO_2 emissions for the United States *Journal of Geophysical Research: Atmospheres* **125** e2020JD032974
Gurney K R, Razlivanov I, Song Y, Zhou Y, Benes B and Abdul-Massih M 2012 Quantification of fossil fuel CO_2 emissions on the building/street scale for a large U.S. city *Environ. Sci. Technol.* **46** 12194–202
Holzworth G C 1964 Estimates of mean maximum mixing depths in the contiguous United States *Mon. Weather Rev.* **92** 235–42
Horel J *et al* 2002 Mesowest: cooperative mesonets in the United States *Bull. Am. Meteorol. Soc.* **83** 211–26
Hutyra L R, Duren R, Gurney K R, Grimm N, Kort E A, Larson E and Shrestha G 2014 Urbanization and the carbon cycle: current capabilities and research outlook from the natural sciences perspective *Earth's Future* **2** 473–95
International Energy Agency 2008 *World Energy Outlook 2008* (International Energy Agency; Turpin Distribution)
Jacobson A R *et al* 2020 Carbon tracker CT2019B, Model published 2020 by NOAA Earth System Research Laboratory, Global Monitoring Division (https://doi.org/10.25925/20201008)
Kunik L *et al* 2019 Bayesian inverse estimation of urban CO_2 emissions: results from a synthetic data simulation over Salt Lake City, UT *Elem Sci Anth* **7** 36
Li Y, Pizerb W A and Wu L 2021 Climate change and residential electricity consumption in the Yangtze River Delta, China *PNAS* **116** 472–7
Lin J C *et al* 2018 CO_2 and carbon emissions from cities -linkages to air quality, socioeconomic activity, and stakeholders in the Salt Lake City Urban Area *Bull. Ameri. Meteoro. Soc.* **99** 2325–39
Lundberg S M *et al* 2020 From local explanations to global understanding with explainable AI for trees *Nat Mach Intell* **2** 56–67
Mallia D V, Mitchell L E, Gonzalez Vidal A E, Wu D, Kunik L and Lin J C 2023 Can we detect urban-scale CO_2 emission changes within medium-sized cities? *Journal of Geophysical Research: Atmospheres* **128** e2023JD038686
McKain K, Wofsy S C, Nehrkorn T, Eluszkiewicz J, Ehleringer J R and Stephens B B 2012 Assessment of ground-based atmospheric observations for verification of greenhouse gas emissions from an urban region *Proc. Natl. Acad. Sci. U.S.A.* **109** 8423–28
Mitchell L E *et al* 2018 Long-term urban carbon dioxide observations reveal spatial and temporal dynamics related to urban characteristics and growth *PNAS* **115** 2912–7
Mourshed M 2012 Relationship between annual mean temperature and degree-days *Energy Build.* **54** 418–25
Nasrallah H A, Balling Jr R C, Madi S M and Al-Ansari L 2003 Temporal variations in atmospheric CO_2 concentrations in Kuwait City, Kuwait with comparisons to Phoenix, Arizona, USA *Environ. Pollut.* **121** 301–5
National Transportation Atlas Databases (NTAD) 2003 United States, Department of Transportation. Bureau of Transportation Statistics www.worldcat.org/title/ntad-2003-a-collection-of-spatial-data-for-use-ingis-based-applications/oclc/52933703?referer=one_hit, accessed July 22, 2012. (https://doi.org/10.21949/1502416)
Nelson D, Choi Y, Sadeghi B, Yeganeh A K, Ghahremanloo M and Park J 2023 A comprehensive approach combining positive matrix factorization modeling, meteorology, and machine learning for source apportionment of surface ozone precursors: underlying factors contributing to ozone formation in Houston, Texas *Environ. Pollut.* **334** 122223
Newman S *et al* 2013 Diurnal tracking of anthropogenic CO_2 emissions in the Los Angeles basin megacity during spring 2010 *Atmos. Chem. Phys.* **13** 4359–72
Nowak D J, Stevens J C, Sisinni S M and Luley C J 2002 Effects of urban tree management and species selection on atmospheric carbon dioxide *J. Aboriculture* **28** 113–22
Parazoo N C, Denning A S, Kawa S R, Corbin K D, Lokupitiya R S and Baker I T 2008 Mechanisms for synoptic variations of atmospheric CO_2 in North America, South America and Europe *Atmos. Chem. Phys.* **8** 7329–7254
Pataki D E, Bowling D R and Ehleringer J R 2003 Seasonal cycle of carbon dioxide and its isotopic composition in an urban atmosphere: anthropogenic and biogenic effects *J. Geophys. Res.* **108** 4735
Pataki D E, Bowling D R, Ehleringer J R and Zobitz J M 2006 High resolution atmospheric monitoring of urban carbon dioxide sources *Geophys. Res. Lett.* **33** L03813
Pataki D E, Tyler B J, Peterson R E, Nair A P, Steenburgh W J and Pardyjak E R 2005 Can carbon dioxide be used as a tracer of urban atmospheric transport? *J. Geophys. Res.* **110** D15102
Patarasuk R, Gurney K R, O'Keeffe D, Song Y, Huang J, Rao P, Buchert M, Lin J C, Mendoza D and Ehleringer J R 2016 Urban high-resolution fossil fuel CO_2 emissions quantification and exploration of emission drivers for potential policy applications *Urban Ecosyst* **19** 1013–39
Pedregosa F, Varoquaux G, Gramfort A, Michel V, Thirion B, Grisel O and Duchesnay E 2011 Scikit-learn: machine learning in python *Journal of Machine Learning Research* **12** 2825–30
Petrick S, Rehdanz K and Tol R S J 2010 The impact of temperature changes on residential energy consumption *Kiel Working paper* **April 2010** No.1618
Ray R L, Singh V P, Singh S K, Acharya B S and He Y 2022 What is the impact of COVID-19 pandemic on global carbon emissions? *Sci. Total Environ.* **816** 151503
Rosenzweig C, Solecki W, Hammer A A and Mehrotra S 2010 Cities lead the way in climate-change action *Nature* **467** 909–11
Ryoo J-M *et al* 2019 Quantification of CO_2 and CH_4 emissions over sacramento, California, based on divergence theorem using aircraft measurements *Atmos. Meas. Tech.* **12** 2949–66
Seidel D J, Ao C O and Li K 2010 Estimating climatological planetary boundary layer heights from radiosonde observations: comparison of methods and uncertainty analysis *J. Geophys. Res.* **115** D16113
Shapley L S 1953 17. A Value for n-person games'. Contributions to the theory of games (AM-28), Volume II ed Harold William Kuhn and Albert William Tucker Princeton(Princeton University Press) 307–18
Strong C, Stwertka C, Bowling D R, Stephens B B and Ehleringer J R 2011 Urban carbon dioxide cycles within the Salt Lake valley: a multiple-box model validated by observations *J. Geophys. Res.* **116** D15307

Turner A, Kim J, Fitzmaurice H, Newman C, Worthington K, Chan K, Wooldridge P J, Koehler P, Frankenberg C and Cohen R C 2020 Observed impacts of COVID-19 on urban CO_2 emissions *Geophys. Res. Lett.* **47** e2020GL090037

Umezawa T, Matsueda H, Oda T, Higuchi K, Sawa Y, Machida T, Niwa Y and Maksyutov S 2020 Statistical characterization of urban CO_2 emission signals observed by commercial airliner measurements *Nature, Scientific Reports* **10** 7963

Vasumathi K K, Nithiya E M, Pandey R and Premalatha M 2017 Studies on the effect of wind speed on loss of carbon dioxide during bio sequestration *Int. J. Hydrogen Energy* **42** 26555–62

Venturi S *et al* 2021 Unveiling the changes in urban atmospheric CO_2 in the time of COVID-19 pandemic: a case study of Florence (Italy) *Sci. Total Environ.* **795** 148877

Wentz E A, Gober P, Balling J R C and Day T A 2002 Spatial patterns and determinants of winter atmospheric carbon dioxide concentrations in an urban environment *Ann. Assoc. Am. Geogr.* **92** 15–28

Wofsy S C *et al* 2010a Measurement requirements for greenhouse gas concentrations in support of treaty monitoring and verification *Eos Trans.* (AGU) Fall Meet. Suppl., Abstract GC41G-04

Wofsy S C, McKain K, Eluszkiewicz J, Nehrkorn T, Pataki D E and Ehleringer J R 2010b An observational method for verifying trends in urban CO_2 emissions using continuous measurements and high resolution meteorology *Eos Trans.* (AGU) Fall Meet. Suppl., Abstract A13F-0280

Wu S, Zhou W, Xiong X, Burr G S, Cheng P, Wang P, Niu Z and Hou Y 2021 The impact of COVID-19 lockdown on atmospheric CO_2 in Xi'an, China *Environ. Res.* **197** 111208

Xueref-Remy I *et al* 2018 Diurnal, synoptic and seasonal variability of atmospheric CO_2 in the Paris megacity area *Atmos. Chem. Phys.* **18** 3335–62

Yadav V *et al* 2021 The impact of COVID-19 on CO_2 emissions in the Los Angeles and Washington DC/Baltimore metropolitan areas *Geophys. Res. Lett.* **48** e2021GL092744

Yin Z, Liu Z, Liu X, Zheng W and Yin L 2023 Urban heat islands and their effects on thermal comfort in the US: New York and New Jersey *Ecol. Indic.* **154** 110765